Mixed desorption of He, H_2, and CH_4 adsorbed on charcoal maximally cooled at 10K

Fukada, Satoshi
Department of Advanced Energy Engineering Science, Kyushu University

Terashita, Masashi
Department of Advanced Energy Engineering Science, Kyushu University

https://hdl.handle.net/2324/26056

出版情報：Journal of Nuclear Science and Technology. 47 (12), pp.1219-1226, 2010-12. 日本原子力学会
バージョン：

[Article]

Mixed desorption of He, H_2, and CH_4 adsorbed on charcoal maximally cooled at 10K

Satoshi FUKADA*, Masashi TERASHITA

Department of Advanced Energy Engineering Science, Kyushu University
Hakozaki, Higashi-ku, Fukuoka 812-8581, Japan

**Corresponding author*
Tel 81-92-642-4140, Fax 81-92-585-6050, Email sfukada@nucl.kyushu-u.ac.jp

Total page: 25 pages
Text page: 13 pages
Table: 1 page
Figures: 12 pages

abstract

Desorption rates of mixtures of He, H_2, and CH_4 adsorbed on activated carbon placed in an enclosed vessel are determined under the condition where the temperature is elevated from 10K to room temperature. Activated carbon is selected because of its good adsorption performance at the cryogenic temperature. The carbon used in the present study is covered with or mesopores or micropores from 1 nm to 10 nm in diameter. The adsorption and desorption of their respective gases proceed independently, and desorption behavior of each component is well expressed in terms of a Langmuir-Freundlich isotherm. Since desorption curves under different heating conditions can be correlated to the same one on a (T-p_i) plot, it is considered that gas desorption proceeds under equilibrium condition between the adsorbent and gaseous phases. Two- or three-component desorption of He, H_2, and CH_4 from activated carbon can be described using an extended multicomponent Langmuir-Freundlich isotherm without any correction. Desorption curves calculated for their respective gases are in comparatively good agreement with experimental data.

Keywords:
cryosoption, activated carbon, tritium, helium, methane, hydrogen

I. Introduction

In a fusion reactor system, the D-T fuel cycle should be established not only to maintain self-sufficient fuel supply but also to meet legal regulations on radiation safety and radiation hygiene, such as the maximum inventory and maximum allowable concentration of tritium in a laboratory room. D-T fuel in a high-temperature plasma chamber is partly burned, and interacts with structural walls such as the first wall and diverter plates. Multicomponent gaseous mixtures including unburned D-T fuel, He, and impurities such as methane, water, and hydrocarbons are exhausted in a lump by evacuation pumps.1,2) Cryosorption pumps for gas evacuation provide an attractive method of recovering the multicomponent gaseous mixture generated in a chamber. All the gases are adsorbed in a lump on an adsorbent cooled at liquid He temperature. The adsorption rate is expected to be very fast, and the ultimate pressure is very low. Therefore, the fuel supply and plasma burning can be operated under clean conditions.3) However, the evacuation process is not continuous because of the limit of the adsorption capacity of the cryosorption pump.1,4) The evacuated gas should be regularly desorbed by heating the saturated cryosorption pump, and the desorbed gas is sent to the following fuel purification process using Pd-Ag membrane tubes and catalyst beds.1,3) The desorption process is intermittently operated. However, it is preferable to supply gas to the following fuel purification process continuously. Therefore, several cryosorption pumps are combined and operated in turn. In addition, it is necessary to use a surge tank in order to operate the fuel purification process smoothly. Although the desorption of various gases proceeds selectively at different temperatures5) according to their respective vapor pressures or interaction energies between adsorbent and adsorbate, the information on selective gas desorption from the adsorbent is lost when the desorption gas is stored in a surge tank together. If the information on the selective gas desorption is efficiently utilized in the following fuel purification process, the scale of the fuel purification process, such as the number of Pd-Ag membrane tubes, can be decreased.

In the present study, the selective desorption from a cryosorption pump is investigated experimentally and analytically. Previously, there was some research to investigate processes of adsorption and desorption of a single component of He or H_2 and two-component mixtures on activated carbon utilized for cryosorption pumps.5,6) In addition, the performance of gas adsorption in a large-scale cryosorption pump was experimentally investigated by the ITER group.7,8) The basic adsorption and desorption mechanism and the isotherm of activated carbon for various gaseous molecules were investigated previously.5,6,8,9) However, there is no analytical or experimental study on the adsorption and desorption behavior of multicomponent gas mixtures on the adsorbent. In the present study, experimental results and analytical equations for the three-component gas adsorption and desorption of He, H_2, and CH_4 are presented. We selected He and CH_4 as representative impurity molecules with high or low vapor pressure that will be generated in plasma chambers and H_2 as a representative of D-T fuel. There is less isotope effect in adsorption or desorption on activated carbon among hydrogen isotopes of H_2, D_2, and T_2.6,7)

II. Experimental

The experimental apparatus is the same as that shown in our previous study.5,6) The vacuum chamber has a volume of 3.2 L. The chamber is composed of three parts; (i) activated carbon adsorbent that is cooled around at 10 K, (ii) a cryopanel part that is cooled at around 10 K, and (iii) a baffle-panel part cooled around at 80 K. Cooling is performed using two-stage cooling units, which can cool maximally down to 10 K. The cryopanel is coated with a thin activated charcoal film as adsorbent. The temperature is measured using Chromel-AuFe (0.07%) thermocouples.

The amount of activated carbon used in the present experiment is 60 g. The specific surface area of the charcoal film is 644 m^2/g, which was determined using a BET specific-surface-area meter (TriStar 3020, Shimadzu corporation). When we use the nitrogen molecular cross-sectional area of 0.162 nm^2, the BET specific surface area corresponds to the adsorption amount of 6.6 mmol/g. **Figure 1** shows the pore volume distribution of activated carbon used in the present study. The vertical axis is presented in terms of the differential of the cumulative adsorbed amount of nitrogen based on the Barrett–Joyner–Halenda (BJH) method.10) Its values correspond to the pore size distribution with the unit of [cm^3(NTP)/g(nm)]. The pore diameter on the horizontal axis, d_p, is calculated using the sum of the Kelvin equation (the first term of Eq. (1)) and the Halsey equation (its second term) as follows:

$$d_p = 2\left[\frac{0.955}{\ln\left(p_0/p\right)} + 0.354\left\{\frac{5}{\ln\left(p_0/p\right)}\right\}^{1/3}\right] \quad [\mathrm{nm}] \qquad (1)$$

Here, the relative nitrogen pressure at liquid nitrogen temperature is defined as p/p_0, in which $p_0 = 1.0133\text{x}10^5$ Pa. The pore volume determined is distributed in the range from 1.5 to 25 nm as seen in the figure. The surface area meter used in the present study cannot be used to detect a pore diameter smaller than 1.5 nm. The figure shows that the activated carbon has a large number of mesopores of around d_p = 3 nm. Therefore, this material is suitable for the adsorption of small molecules of He and H_2 at the cryogenic temperature.

The total pressure of the vacuum chamber is detected using two absolute-pressure gauges

(Baratron capacitance manometers, MKS Instruments). The different ranges of manometers make it possible to measure at a range from 10^{-3} to 10^{3} Pa. Another ionization gauge is used to detect pressure under vacuum. The ultimate pressure measured in the system is 10^{-5} Pa. A mechanical booster pump (MBS 303, ULVAC corporation) is used for roughing evacuation. The residual gas is measured using a quadrupole mass spectrometer (BGM-101, ULVAC), which is evacuated using a turbomolecular pump (UTM-150, ULVAC). In order to keep the material balance correctly, however, the residual gas meter and ionization gauge were not used during the desorption experiment. The total pressure only is measured using the capacitance manometer during the temperature elevation for gas desorption. The residual gas is analyzed before and after the temperature elevation.

An experiment is performed using the following procedures: (i) A vacuum chamber is evacuated using the mechanical booster pump. (ii) A single component of He, H_2, or CH_4 or a two- or three-component mixture is introduced under conditions of a specified partial (and total) pressure and room temperature. (iii) Cooling of the cryosorption pump is started, and the total pressure and temperature are recorded. (iv) After the system has been sufficiently cooled to 10 K and the pressure has achieved a steady-state ultimate value, cooling of the cryosorption pump is cut off. (v) The increments of temperature and total pressure are recorded. No gas evacuation is carried out during the temperature elevation period. (vi) The temperature elevation is controlled using a band heater curled around the shell of the cryosorption pump. The temperature of the heater can be elevated maximally at 70°C. (vii) Desorbed gas in the system is analyzed using the quadrupole mass spectrometer. (viii) Then, the experiment of adsorption and desorption is repeated under another experimental condition.

III. Analysis

1. Material balance in evacuation vessel

Under an initial condition before cooling, an enclosed chamber volume v is filled with an ideal gas mixture of k-component partial pressure, $p_{k,0}$ (k = He, H_2 and CH_4), and temperature of T_{room}. The molar amount $n_{k,0}$ for each of the k components is determined as follows:

$$\frac{p_{k,0}v}{R_g T_{room}} + M_{ad} q_k\left(T_{room}, p_{He,0}, p_{H_2,0}, p_{CH_4,0}\right) = n_{k,0} \quad (k = \mathrm{He}, \mathrm{H_2}, \text{ and } \mathrm{CH_4}) \quad (2).$$

The total molar amount of gas introduced initially in the chamber, $n_{t,0}$, and the total pressure, $p_{t,0}$, are the sum of each component as follows:

$$n_{t,0} = n_{He,0} + n_{H_2,0} + n_{CH_4,0} \qquad (3),$$

$$p_{t,0} = p_{He,0} + p_{H_2,0} + p_{CH_4,0} \quad (4).$$

When the chamber is evacuated using a cryosorption pump, the material balance of the mixed gaseous components in the enclosed chamber and pump at arbitral temperature of T is described as follows:

$$\frac{p_k v_C}{R_g T} + \frac{p_k\left(v - v_C\right)}{R_g T_{room}} + M_{ad} q_k\left(T, p_{He}, p_{H_2}, p_{CH_4}\right) = n_{k,0} \quad (k = \mathrm{He}, \mathrm{H_2}, \text{and } \mathrm{CH_4}) \ (5).$$

The total pressure under the arbitral cooled condition, p_t, is the sum of the partial pressures for each component under respective conditions as follows:

$$p_t = p_{He} + p_{H_2} + p_{CH_4} \quad (6).$$

The molar fraction of the k component at the arbitral cooled condition, x_k, and its value at the initial condition, $x_{k,0}$, are defined as follows:

$$x_k = \frac{p_k}{p_t} \quad (k = \mathrm{He}, \mathrm{H_2}, \text{and } \mathrm{CH_4}) \quad (7),$$

$$x_{k,0} = \frac{p_{k,0}}{p_{t,0}} \quad (k = \mathrm{He}, \mathrm{H_2}, \text{and } \mathrm{CH_4}) \quad (8).$$

For the activated carbon used in the present study, the second term on the left-hand side in Eq. (2) is negligibly small. Therefore, the term is regarded as zero in the analysis described below. Thus, the combination of Eqs. (1)-(7) results in the equation:

$$\left(\frac{1}{T_R}\frac{v_C}{v} + \frac{v - v_C}{v}\right) p_R x_k + \frac{M_{ad}}{n_{t,0}} q_k\left(T, p_{He}, p_{H_2}, p_{CH_4}\right) = x_{k,0} \quad (k = \mathrm{He}, \mathrm{H_2}, \text{and } \mathrm{CH_4}) \ (9),$$

where p_R and T_R are the normalized total pressure and temperature defined as follows:

$$p_R = \frac{p_t}{p_{t,0}} \quad (10),$$

$$T_R = \frac{T}{T_{room}} \quad (11).$$

Thus, the dimensionless pressure and temperature are normalized using their respective values under the initial condition and are defined in the ranges of $0 \le p_R \le 1$ and $0 \le T_R \le 1$.

2. Single-component adsorption and desorption

When a single component gas is initially introduced in the cryosorption pump, the values of x_k and $x_{k,0}$ are always equal to unity in Eq. (8). Consequently, the following material balance equation of a single component in the enclosed chamber is valid:

$$\frac{M_{ad}}{n_{t,0}} q_k\left(T, p_k\right) = 1 - p_R\left(\frac{1}{T_R}\frac{v_C}{v} + \frac{v - v_C}{v}\right) \quad (k = \mathrm{He}, \mathrm{H_2}, \text{and } \mathrm{CH_4}) \quad (12).$$

When equilibrium is achieved between a gas phase and an adsorbed phase, $q_k(T,p_{k,})$ is described using an adsorption isotherm. Then, the adsorption (or desorption) isotherm for each single component, $q_k(T,p_k)$, can be determined from the experimental (T-p_k) relation (or the normalized (T_R-p_R) relation) and Eq. (12). It is assumed in the present study that the adsorption (or desorption) isotherm of the single component, $q_k(T,p_k)$, can be correlated to the Langmuir-Freundlich relation proposed by Sips: [11)]

$$q_k(T,p_k) = q_{k,\infty}\frac{K_k p_k^{n_k}\exp\left(\frac{E_k}{R_g T}\right)}{1+K_k p_k^{n_k}\exp\left(\frac{E_k}{R_g T}\right)} \qquad (k = \mathrm{He},\ \mathrm{H_2},\ \text{and } \mathrm{CH_4}) \qquad (13).$$

The experimental history of an adsorption-desorption process on the (T-p_k) plane and the combination of Eqs. (12) and (13) can give the values of the parameters included in the adsorption (or desorption) isotherm of Eq. (13), K_k, E_k and n_k. The values determined for He, H_2, and CH_4 are given in **Table 1**.

3. Multicomponent adsorption and desorption

The above single-component isotherm, Eq. (13), is extended to the case of multicomponent adsorption. For the multicomponent adsorption or desorption of gaseous mixtures composed of He, H_2, and CH_4, the following extended Langmuir-Freundlich relation is assumed here:

$$q_k(T,p_{He},p_{H_2},p_{CH_4}) = q_{k,\infty}\frac{K_k p_k^{n_k}\exp\left(\frac{E_k}{R_g T}\right)}{1+K_{He} p_{He}^{n_{He}}\exp\left(\frac{E_{He}}{R_g T}\right)+K_{H_2} p_{H_2}^{n_{H_2}}\exp\left(\frac{E_{H_2}}{R_g T}\right)+K_{CH_4} p_{CH_4}^{n_{CH_4}}\exp\left(\frac{E_{CH_4}}{R_g T}\right)}$$

$$(k = \mathrm{He},\ \mathrm{H_2}\ \text{and } \mathrm{CH_4}) \qquad (14).$$

Eq. (14) is deduced from a material balance on the surface under the condition where three gases are adsorbed on the same site and there is no interaction among the adsorbed gases except for combining energy between the adsorbent and adsorbate. When competitive adsorption proceeds among a multicomponent gaseous mixture, the adsorption amount of the k component is a function of not only the partial pressure of the corresponding k component but also those of other components. There is no additional parameter in Eq. (14) except the parameters determined from each isotherm of a single component. In other words, there is no correction in Eq. (14), and the isotherm of multicomponent mixtures can be determined automatically from that of the single component.

If each of gases adsorbed and desorbed behaves independently, the isotherm for the three-component mixture of He, H_2 and CH_4, Eq. (14), can be approximated using the following simplified equation similar to a single-component isotherm:

$$q_k\left(T,p_t,x_k\right)=q_{k,\infty}x_{k,0}\frac{K_k p_t^{n_k} x_k^{n_k}\exp\left(\frac{E_k}{R_g T}\right)}{1+K_k p_t^{n_k} x_k^{n_k}\exp\left(\frac{E_k}{R_g T}\right)} \qquad (k = \text{He}, H_2, \text{and } CH_4) \qquad (15).$$

IV. Results and Discussion

1. Single-component desorption

Figure 2 shows experimental data for the desorption of a single component gas (He, H_2, or CH_4) adsorbed on activated carbon in the process of heating from 10 K to room temperature. The vertical axis is pressure and the horizontal axis is temperature. The left and bottom values are normalized using appropriate respective initial conditions, and the right and top ones are raw values. The initial pressure of gas introduced to the chamber is constant ($p_{t,0}$ = 100 Pa) throughout the present experiment. When the adsorbed gas has been completely desorbed during the temperature elevation, each desorption curve approaches a single nonadsorption curve, which means $q_k(T,p_k)=0$ in Eq. (5) or (9). Consequently, the relation of $1-\left(p_r\right)_{nonadsorption}\left(\frac{1}{T_r}\frac{v_C}{v}+\frac{v-v_C}{v}\right)=0$ from Eq. (9) is obtained under the nonadsorption condition. The nonadsorption curve shown by a broken line in the figure is independent of gaseous species in the case of ideal gas. The adsorbed amount on the activated carbon can be determined from the difference between the nonadsorption and adsorption conditions.

Figures 3(a) and **(b)** comparatively show desorption curves for two different temperature elevation rates for He and CH_4, respectively. The desorption proceeds differently for each gas depending on the temperature elevation rate. Since the limit of the maximum allowable temperature of welding used in the present cryosorption pump is 70°C, the temperature elevation rate cannot be changed widely. The gas amount adsorbed per unit activated carbon remains constant immediately after the temperature elevation, because the gas amount introduced to the chamber is constant as $n_{k,0}$ = $1.31\text{x}10^{-4}$ mol (2.95 cm^3 (NTP)) for any k component (k = He, H_2, and CH_4) throughout the experiment. When desorption is initiated, the amount adsorbed on charcoal decreases according to the temperature elevation.

The adsorbed amounts for the two different heating rates are plotted as a function of temperature in **Fig. 4**. As seen in the figure, there are hardly any changes in the desorption curves regardless of the different temperature increment rates. This tendency was the same for gases of He, H_2, and CH_4. This is because the desorption proceeds under an equilibrium condition. Therefore, we can determine the isotherm of $q_k(T,p_k)$ from a desorption history during the heating process.

Figure 5 shows the normalized adsorption amount on the left axis, $M_{ad}q_k(T,p_k)/n_{t,0}$, as a function of the normalized temperature on the bottom axis, T_R. The values of respective raw data are on the right axis and the top axes. Almost every gas introduced in the system is adsorbed at the cryogenic temperature. Consequently, the p_R value becomes zero when T_R is very low, as seen in Fig. 2. Therefore, the $M_{ad}q_k(T,p_k)/n_{t,0}$ value of Fig. 5 becomes unity when T_R approaches zero. On the other hand, p_R becomes unity from the initial condition when T_R approaches unity, and therefore, the $M_{ad}q_k(T,p_k)/n_{t,0}$ value becomes zero. The values of the parameters included in the isotherm were determined for their respective gases from fitting calculations to the experimental data of Fig. 5 and are tabulated in **Table 1**. The pressure dependence for He desorption is determined based on previous studies of He adsorption isotherm on activated carbon,[12,13)] the pressure index in the isotherm for He, n_{He}, is assumed to be 0.2. The pressure index for the H_2 or CH_4 adsorption is assumed to be unity in this pressure region judging from previous papers.[14,15)] The adsorption heat is almost coincident with previous studies.[12-16)]

2. Multi-component desorption

The 2- or 3-component gaseous mixtures of He, H_2, and CH_4 with specified compositions are introduced into the vacuum chamber at a total pressure of $p_{t,0}$ (100 Pa) and are cooled. **Figures 6(a), 6(b) and 6(c)** show variations of the normalized total adsorption amount of $M_{ad}q_t(T,p_{He}, p_{H2}, p_{CH4})/n_{t,0}$ on the left axis with T_R on the bottom axis for different combinations of the two-component gas mixtures. The values of the right and top axes are original data before normalization. The broken lines are calculation results using Eq. (14). **Figure 7** shows variations of the $M_{ad}q_t(T,p_{He}, p_{H2}, p_{CH4})/n_{t,0}$ value on the left axis with T_R on the bottom axis for the three-component gas mixtures. The initial molar fraction of $x_{k,0}$ and the initial partial pressure of $p_{k,0}$ are determined from pressure change when each gas is introduced. The initial molar fraction was coincident with the values measured by the mass spectrometer after gas desorption. Regardless of the combinations of He, H_2, and CH_4, comparatively good agreement is obtained between experiment and calculation. The temperatures at the time when desorption starts are 20 K for He, 75 K for H_2, and 180 K for CH_4, and are independent of the presence of other gas components. The coverage of the adsorption site in the present experiment is estimated around at $3x10^{-4}$. The behavior of independent adsorption may come from the small coverage. Application of the single-component Langmuir-Freundlich isotherm to the multicomponent one can be made without introduction of any additional parameter. Small differences seen in the comparison between the experiment and calculation in Figs. 5(a), 5(b), 5(c) and 6 will be clarified in a future experiment carried out under wider range conditions.

Figure 8 shows desorption rates, dp_R/dt, which are determined from the differential of experimental pressure change. The three peaks seen in the rate curve correspond to the gas desorptions of He, H_2, and CH_4. This figure clearly shows how the three gases are desorbed independently. As a result of numerical fitting, it was found that the desorption rate for the three-component gas mixtures can be approximated by the combination of three Gaussian distribution curves as follows:

$$\frac{dp_t}{dT} = \sum_{k=He,H_2,CH_4} \frac{p_{k,\infty}}{\sqrt{2\pi}\sigma_k} \exp\left[-\frac{(T-T_k)^2}{2\sigma_k^2}\right] \tag{16}$$

In addition, the relation of $\frac{dp_k}{dt} = \left(\frac{dp_k}{dT}\right)\left(\frac{dT}{dt}\right)$ is used for the calculation on the (dp_R/dt-T) plot. All those results indicate that He, H_2, and CH_4 are adsorbed and desorbed on activated carbon at the cryogenic temperature independently.

3. Release of residual gas by heating

It is important to study how other residual gaseous components affect adsorption or desorption on activated carbon. The effect of residual gas is especially important for tritium evacuation.[17] An experiment to investigate the effect of residual gas on the adsorption and desorption of a multicomponent gas is carried out under the following condition. The cryosorption pump is supplied with a mixture of He 50 Pa and CH_4 50 Pa at room temperature, the system is then cooled to 10 K, and the multicomponent gas is desorbed during temperature elevation until room temperature. Next, the desorbed gas is evacuated to 10^{-1} Pa using the mechanical booster pump for roughing evacuation. Then, 100 Pa H_2 is supplied at room temperature. The system is cooled in a similar way and is desorbed by temperature elevation up to 50°C using the band heater. The desorption curve during the last heating process is shown in **Fig. 9** on a logarithmic scale.

As seen in the figure, at first, a small He peak and then a large H_2 peak appear with temperature elevation. The peak area of He is around 1/200 of that of H_2. Then, the peaks of CH_4, N_2, and O_2 emerge at around 150K. The peak of CH_4 is a little larger than that of He. This is because a small amount of CH_4 remained in the adsorbed site of the activated carbon at room temperature regardless of evacuation using the external roughing pump. In the latter desorption process, the system is not evacuated from the outside. Consequently, there is possibility that a small amount of CH_4 is still adsorbed on the activated carbon at room temperature. It was found that the residual CH_4 amount corresponds to around one percent of the supplied gas. The CH_4 supplied initially is desorbed following temperature elevation up to room temperature. N_2 and O_2 are also desorbed in the same temperature range. The peak ratio of N_2:O_2 is around 4:1, and therefore it is considered that their origin comes from a small air leak from the outside. On the other hand, He, H_2, O_2, and N_2 peaks do not show any increase after the temperature elevation until 50°C. Heating above 70°C is not allowed in the present experiment, because of the protection of the thermocouples used here. The adsorption forces of these molecules to the activated carbon are very weak. CH_4 shows a small increase after heating. H_2O is the main molecule that shows a certain increase in the residual gas during heating. The H_2O peak apparently increases after the temperature elevation. Therefore, the main residual gas component remaining on the activated carbon is considered to be H_2O. Our result that H_2O remains on the activated carbon coincides with the previous research by Day *et al.*18) A certain amount of H_2O remains even after room temperature. Therefore pretreatment heating at around 250°C and evacuation by another roughing pump17) are necessary to remove a small amount of H_2O adsorbed on the activated carbon.

V. Conclusions

He, H_2, and CH_4 were independently adsorbed and desorbed on activated carbon from 10 K to room temperature. Their desorption isotherms for single-component, two-component and three-component gases are expressed using an extended Langmuir-Freundlich isotherm. The multicomponent desorption profiles of He, H_2, and CH_4 were predicted comparatively correctly based on the single-component adsorption isotherm. The activated carbon including a pore volume of around 1 nm works well for He and H_2 adsorption at the cryogenic temperature. Selective desorption behavior by a cryosorption pump can be utilized for the simple separation of plasma exhaust gas including unburned fuel, He and impurities before sending the exhaust gas to the following fuel purification system of a fusion reactor system. Although residual gases of CH_4, N_2, and O_2 were observed during temperature elevation to room temperature, those gases can be desorbed by using the external evacuation pump. Heating of the cryosorption pump until 250°C is necessary for the complete desorption of H_2O preadsorbed on activated carbn.

Nomenclature

E_k adsorption heat for *k* component [J/mol]

K_k adsorption constant in equilibrium isotherm for *k* component [1/Pa^n]

M_{ad}	amount of adsorbent [kg]
n_k	molar amount of k component [mol] or index in adsorption isotherm [-]
p_k	partial pressure for k component [Pa]
p_t	total pressure [Pa]
q_k	adsorption amount of k component [mol/kg]
$q_{k,oo}$	adsorption amount under saturated condition [mol/kg]
R_g	gas law constant [J/molK]
T	temperature [K]
T_k	representative desorption temperature for k component [K]
v	total volume of chamber [m^3]
v_C	volume of cooled part [m^3]
x_k	molar fraction of k component [-]
σ_k	standard deviation for k component [K]

Subscripts

k	gaseous component
R	relative condition to initial one
0	initial condition
room	room condition

Acknowledgements

This research is financially supported partly by Grants-in-Aids for Scientific Research in Priority Area on Tritium Science and Technology for Fusion Reactor (contract no. 19055006) and partly by Large Helical Device Coordinated Research of National Institute for Fusion Science (contract no. NIFS07KOBS010).

References

1) M. Glugla, D. K. Murdoch, A. Antipenkov, S. Beloglazov, I. Cristescu, I.-R. Cristescu, C. Day, R. Laesser, A. Mack, “ITER fuel cycle R&D: Consequences for the design”, *Fusion Eng. Des.*, **81** (2006) 733-744.

2) C. Day, A. Mack, M. Glugla, D. K. Murdoch, “Tritium inventories in the high vacuum pumps of ITER”, *Fusion Sci. Technol.*, **41** (2002) 602-606.

3) C. Day, D. Murdoch, “The ITER vacuum systems”, *J. Phys. Conf. Series*, **114** (2008) 012013.

4) M. Wykes, "Minimization of the hydrogenic inventory of the ITER neutral beam line and torus cryosorption pumps", *Fusion Sci. Technol.*, **48** (2005) 39-42.

5) S. Fukada, M. Terashita, "Behavior of desorption of hydrogen, helium and impurities from cryosorption pump", *Fusion Sci. Technol.*, **57** (2010) 112-119.

6) M. Terashita, S. Fukada, "Experimental clarification on desorption behavior of H_2, D_2 and He mixtures from cryo-sorption pump", the result was presented in ICFRM-14 and the paper is contributed to *J. Nucl. Mater.*

7) C. Day, D. Brennan, P. Camp, H. S. Jensen, G. Jones, A. Mack, A. Miller, "Performance of ITER-relevant cryopump panel for triated gases", *Fusion Sci. Technol.*, **48** (2005) 29-34.

8) C. Day, "The use of active carbons as cryosorbent", *Colloids and Surfaces*, **187-188** (2001) 187-206.

9) K. Mohanty, D. Das, M. N. Biswas, "Preparation and characterization of activated carbons from *sterculia alata* nutshell by chemical activation with zinc chloride to remove phenol from wastewater", *Adsorption*, **12** (2006) 119-132.

10) R. T. Yang, "*Adsorbents: fundamentals and applications*", John Wiley and Sons, (2003).

11) R. Sips, "On the structure of a catalytic surface", *J. Chem. Phys.*, **16** (1948) 490-495.

12) M. Kumita, J. Ozaki, J. Kobayashi, M. Ito, F. Watanabe, M. Hasatani, "Characteristics of helium adsorption on microporous solids under cryogenic conditions", *J. Chem. Eng. Japan*, **28** (1995) 159-164.

13) N. Setoyama, K. Kaneko, F. Rodriguez-Reinoso, "Ultramicropore characterization of microporous carbons by low-temperature helium adsorption", *J. Phys. Chem.*, **100** (1996) 10331-10336.

14) L. L. Vasiliev, L. E. Kanonchik, A. G. Kulakov, D. A. Mishkins, P. Brovka, "Activated carbon and hydrogen adsorption storage", *Hydrogen materials science and chemistry of carbon nanomaterials*, (2007) 633-651.

15) F. V. S. Lopes, C. A. Grande, A. M. Ribeiro, J. M. Loureiro, O. Evaggelos, V. Nikolakis, A. E. Rodrigues, "Adsorption of H_2, CO_2, CH_4, CO, N_2 and H_2O in activated carbon and zeolite for hydrogen production", *Sep. Sci. Technol.*, **44** (2009) 1045-1073.

16) Y. Kawamura, M. Enoeda, R. S. Willms, P. M. Zielinski, R. H. Wilhelm, M. Nishi "Adsorption isotherms for tritium on various adsorbents at liquid nitrogen temperature", *Fusion Technol.*, **37** (2000) 54-61.

17) A. I. Vedeneev, M. V. Glagolev, N. T. Kazakovskiy, V. N. Labanov, I. L. Malkov, S. A. Pimanikhin, G. L. Saksaganskiy, "Research into tritium impact on the models of cryosorption panels under conditions simulating operation of a vacuum pump of fusion reactors", *Fusion Eng.*

Des., **58-59** (2001) 355-357.

18) C. Day, B. Kammerer, A. Mack, “The influence of water on the performance of ITER cryosorption vacuum pumps”, *Fusion Eng. Des.*, **51-52** (2000) 229-235.

Table 1 Adsorption parameters of Langmuir-Freundlich isotherm for He, H_2, and CH_4

	He	H_2	CH_4
n_k	0.2	1.0	1.0
E_k	1.75kJ/mol	14.0kJ/mol	44.8kJ/mol
K_k	$1.97\text{x}10^{-3}$ $\text{Pa}^{-0.2}$	$6.16\text{x}10^{-9}$ Pa^{-1}	$5.49\text{x}10^{-12}$ Pa^{-1}

Figure Captions

Fig. 1 Pore volume distribution of activated charcoal

Fig. 2 Variations of pressure and temperature for gas desorption from cryosorption pump

Fig. 3 Desorption curves under different temperature increase conditions

Fig. 4 Gas desorption profiles from activated carbon under different heating conditions

Fig. 5 Experimental desorption profiles for He, H_2, and CH_4 from activated carbon and curves calculated from Langmuir-Freundlich isotherm

Fig. 6(a) Desorption of H_2+He mixtures from activated charcoal

Fig. 6(b) Desorption of He+CH_4 mixtures from activated carbon

Fig. 6(c) Desorption of H_2+CH_4 mixtures from activated carbon

Fig. 7 Desorption of He+H_2+CH_4 mixtures from activated carbon

Fig. 8 Desorption rates of He, H_2 and CH_4 mixtures from active carbon

Fig. 9 Release of residual gas from activated carbon during heating

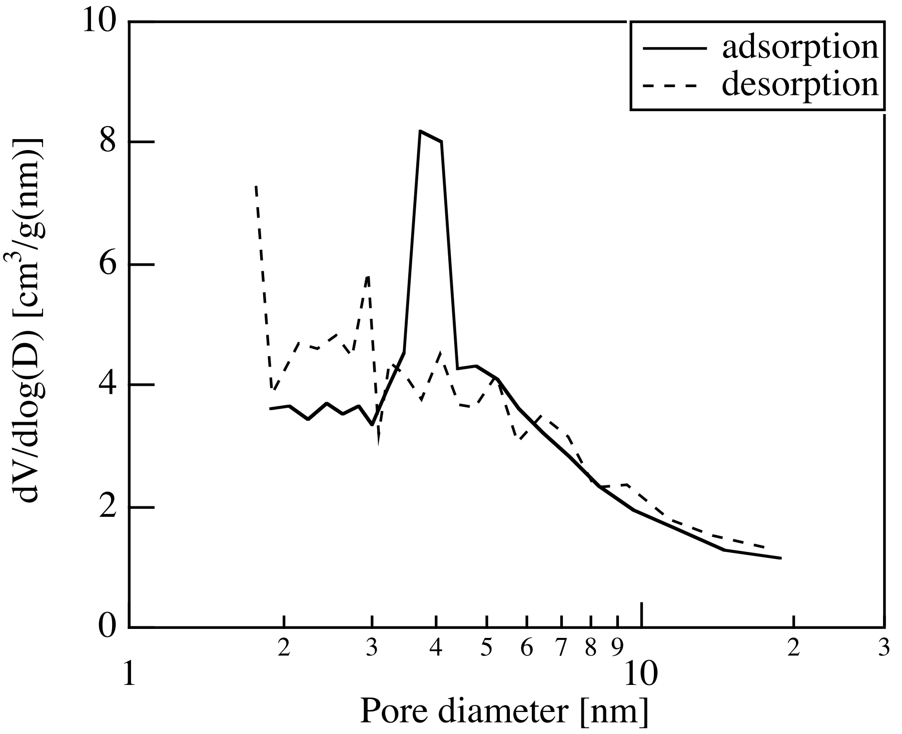

Fig. 1 Pore volume distribution of activated carbon

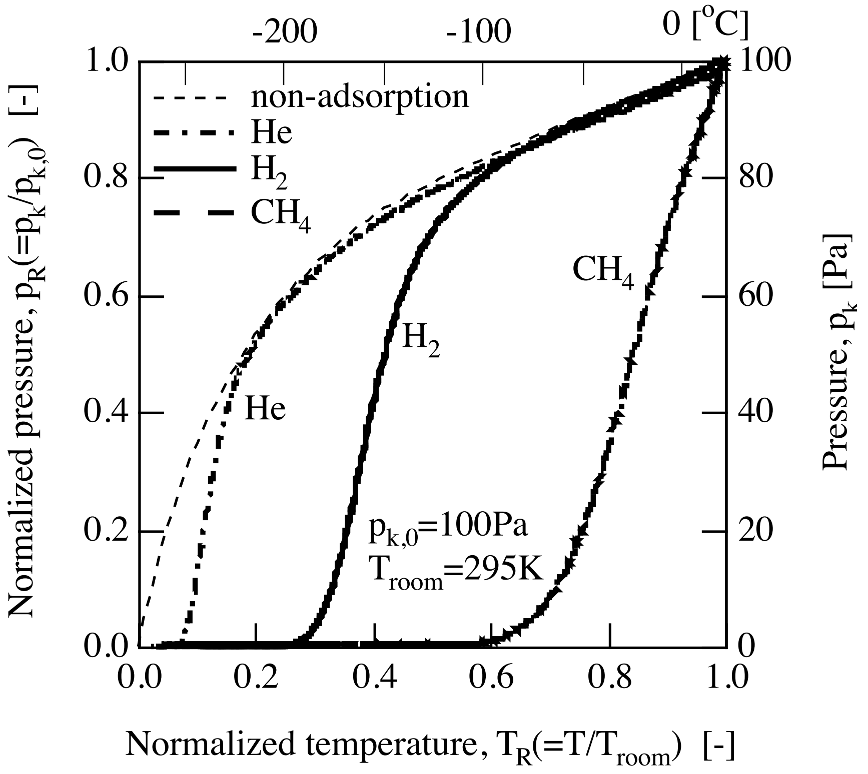

Fig. 2 Variations of pressure and temperature for gas desorption from cryosorption pump

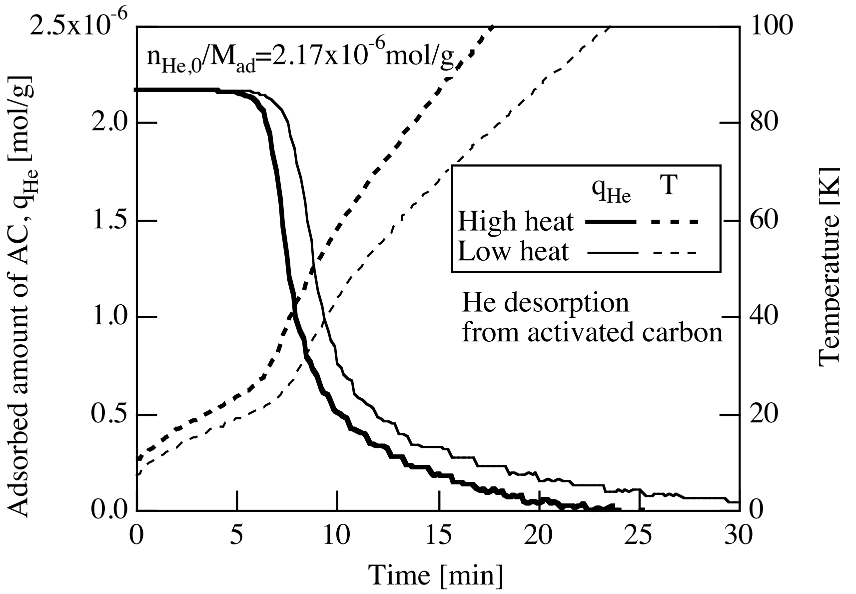

(a) He desorption curves

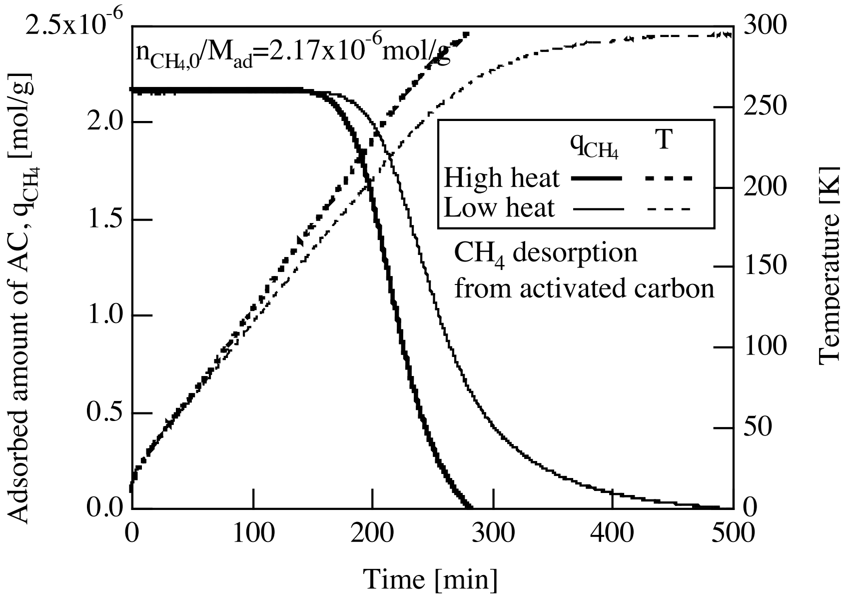

(b) CH_4 desorption curves

Fig. 3 Desorption curves under different temperature increase conditions

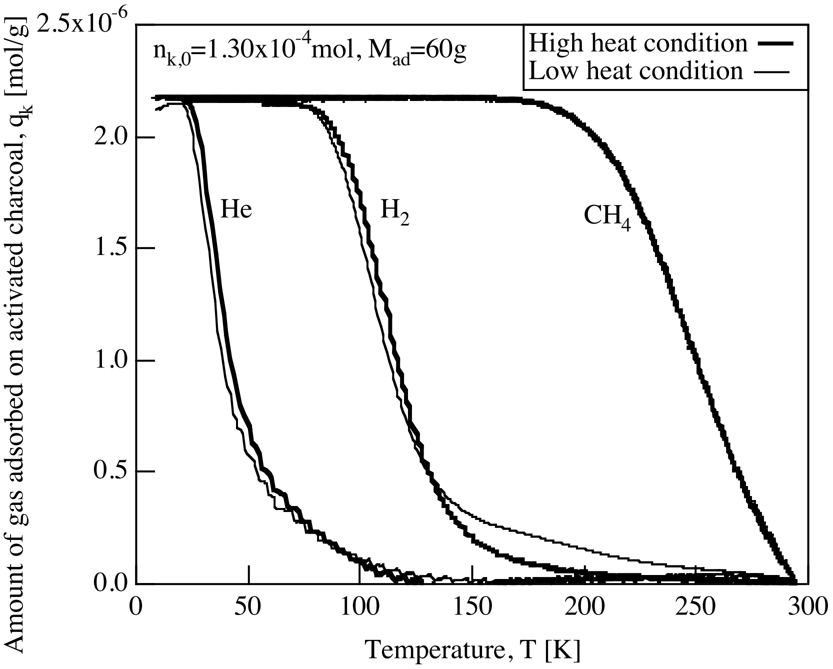

Fig. 4 Gas desorption profiles from activated carbon for different heating conditions

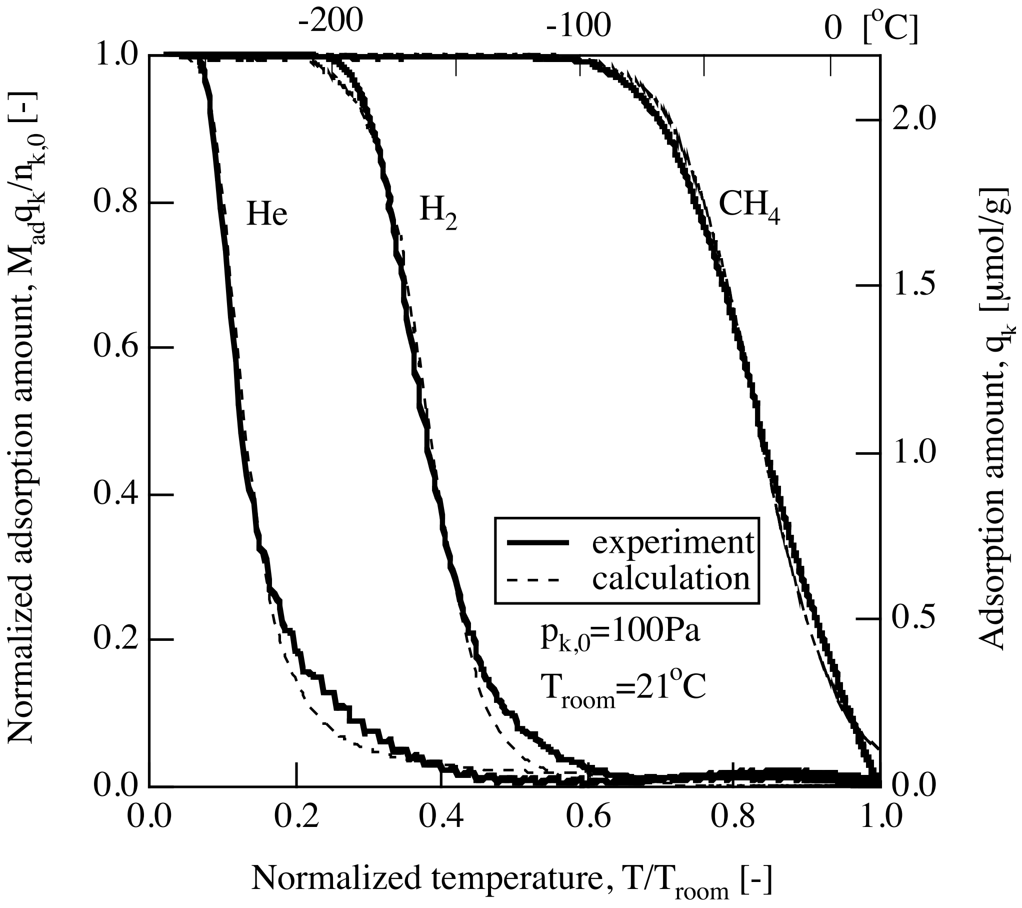

Fig. 5 Experimental desorption profiles for He, H_2, and CH_4 from activated carbon and curves calculated from Langmuir-Freundlich isotherm

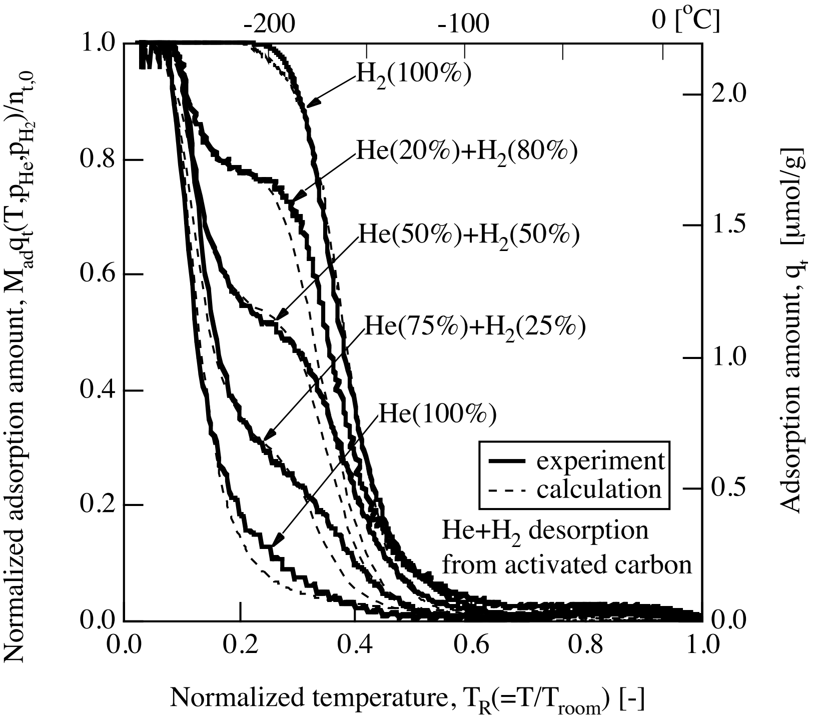

Fig. 6(a) Desorption of H_2+He mixtures from activated carbon

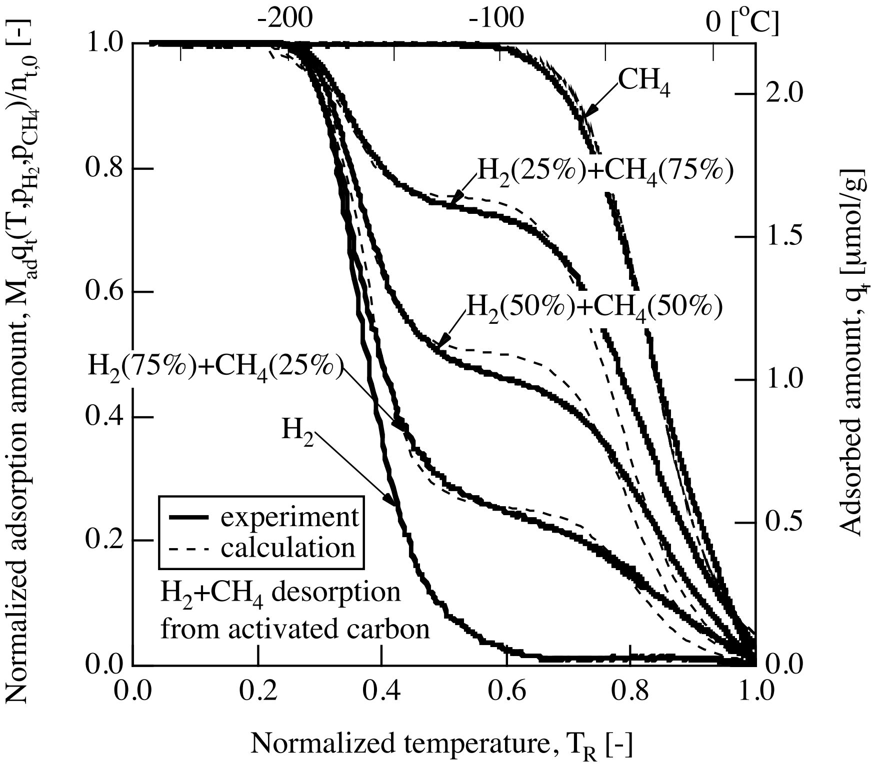

Fig. 6(b) Desorption of He+CH$_4$ mixtures from activated carbon

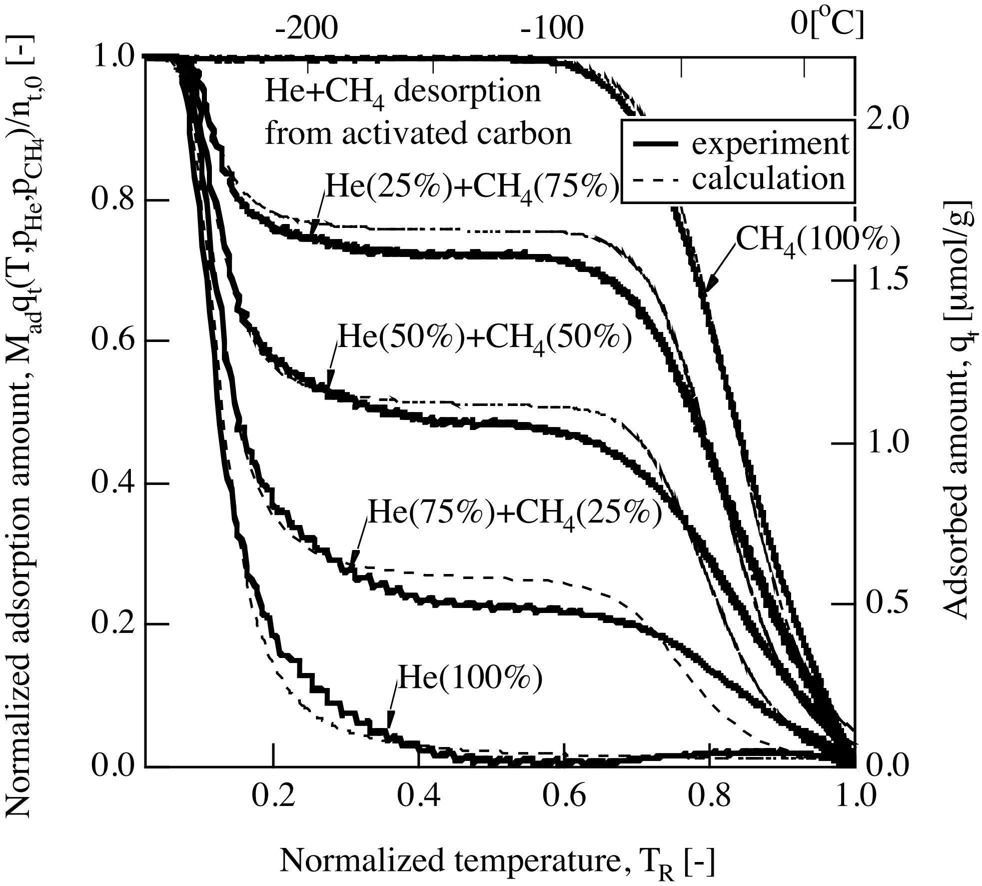

Fig. 6(c) Desorption of H_2+CH_4 mixtures from activated carbon

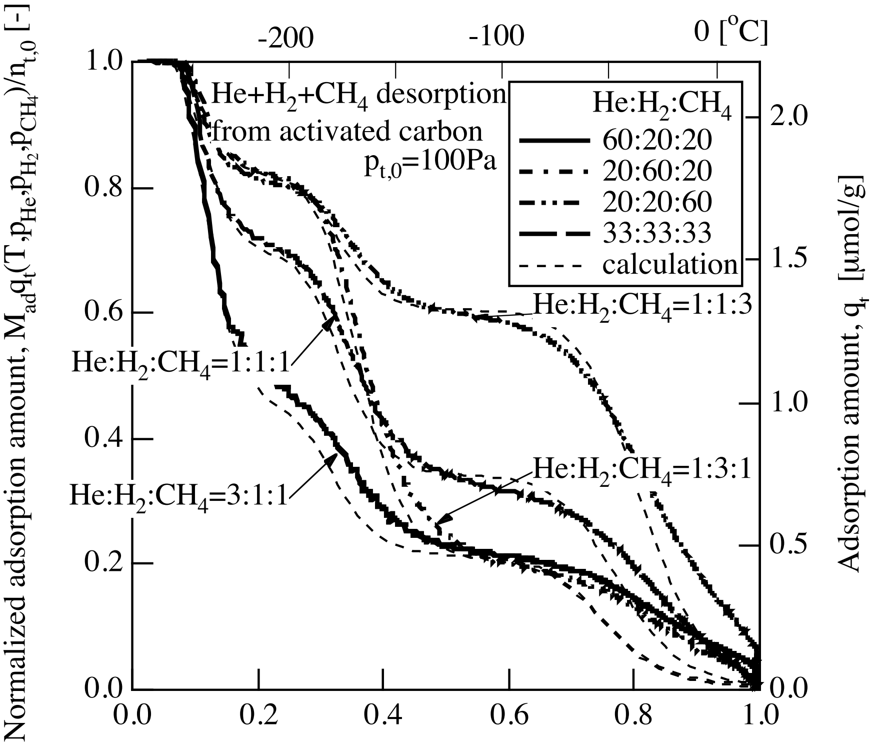

Fig. 7 Desorption of He+H_2+CH_4 mixtures from activated carbon

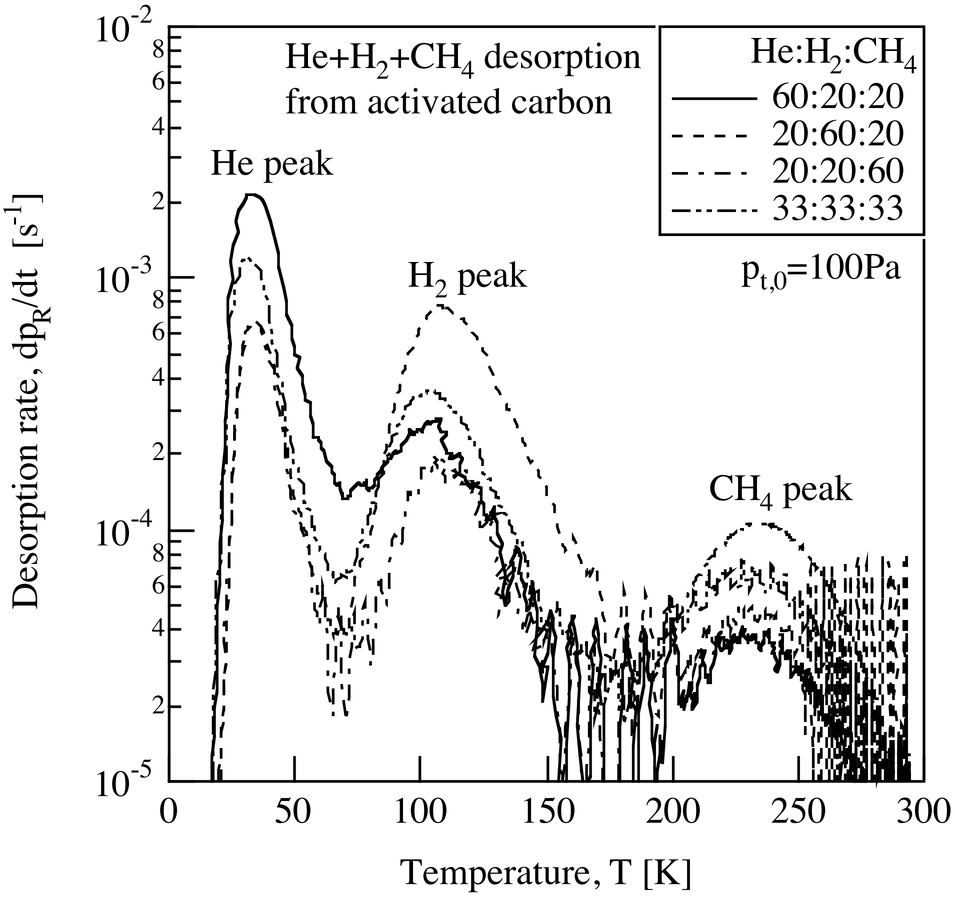

Fig. 8 Desorption rates of He, H_2 and CH_4 mixtures from active carbon

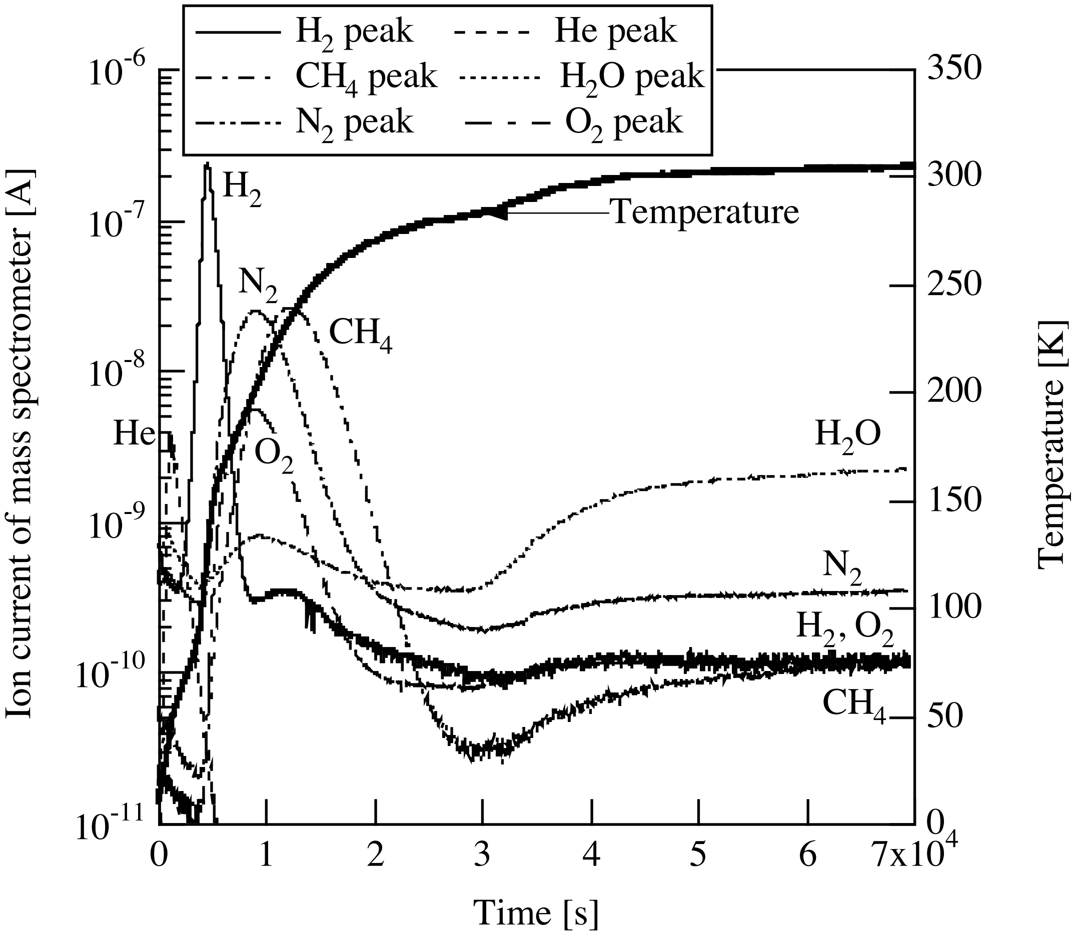

Fig. 9 Release of residual gas from activated carbon during heating